Journal of Pharmaceutical Analysis 2014;4(1):14–25

Contents lists available at ScienceDirect

Journal of Pharmaceutical Analysis

www.elsevier.com/locate/jpa
www.sciencedirect.com

ORIGINAL ARTICLE

Identification of metabolites of *Radix Paeoniae Alba* extract in rat bile, plasma and urine by ultra-performance liquid chromatography–quadrupole time-of-flight mass spectrometry

Zheng-Wei Chen[a,b], Ling Tong[b], Shu-Ming Li[b,c], Dong-Xiang Li[b], Ying Zhang[b], Shui-Ping Zhou[a,b,c], Yong-Hong Zhu[b,*], He Sun[a,b,c]

[a]*Department of Pharmaceutical Analysis, China Pharmaceutical University, Nanjing 210009, China*
[b]*Tasly R&D Institute, Tianjin Tasly Group Co., Ltd., Tianjin 300402, China*
[c]*Center of Drug Metabolism and Pharmacokinetics, China Pharmaceutical University, Nanjing 210009, China*

Received 30 January 2013; accepted 24 June 2013
Available online 18 July 2013

KEYWORDS

Radix Paeoniae Alba;
Metabolite profiling;
UPLC–Q-TOF/MS;
Monoterpene glycosides

Abstract Ultra-performance liquid chromatography coupled with quadrupole time-of-flight tandem mass spectrometry (UPLC–Q-TOF/MS) was developed to identify the absorbed parent components and metabolites in rat bile, plasma and urine after oral administration of *Radix Paeoniae Alba* extract (RPAE). A total of 65 compounds were detected in rat bile, plasma and urine samples, including 11 parent compounds and 54 metabolites. The results indicated that glucuronidation, hydroxylation and methylation were the major metabolic pathways of the components of RPAE. Furthermore, the results of this work demonstrated that UPLC–Q-TOF/MS combined with MetaboLynx™ software and mass defect filtering (MDF) could provide unique high throughput capabilities for drug metabolism study, with excellent MS mass accuracy and enhanced MS^E data acquisition. With the MS^E technique, both precursor and fragment mass spectra can be simultaneously acquired by alternating between high and low collision energy during a single chromatographic run.

*Corresponding author. Tel.: +86 22 86342843; fax: +86 22 86342841.
E-mail address: zyhtasly@163.com (Y.-H. Zhu).

Peer review under responsibility of Xi'an Jiaotong University.

Production and hosting by Elsevier

1. Introduction

Radix Paeoniae Alba, the roots of plant *Paeonia lactiflora* Pall (Family Ranunculaceae), referred as Baishao in China, is a commonly used medicinal herb in traditional Chinese medicine (TCM). Modern phytochemical and pharmacological studies have shown that the major bioactive components of *Radix Paeoniae* are

2095-1779 © 2013 Xi'an Jiaotong University. Production and hosting by Elsevier B.V. Open access under CC BY-NC-ND license.
http://dx.doi.org/10.1016/j.jpha.2013.06.004

monoterpene glycosides, galloyl glucoses and phenolic compounds [1–3]. It displays a range of pharmacological activities such as anti-inflammatory [4], anti-oxidant [5], antiallergic [6], anti-thrombosis [7], immunoregulating [8], cognition-enhancing [9], antihyperglycemic effects [10] and kidney protection effect in diabetic rats [11].

The components of RPAE have been identified thoroughly *in vitro* [12–15]. Li et al. [16] have identified 40 components in RPAE with UPLC–Q-TOF/MS. As the analytical method in Li's [16] research was well developed to identify the components in RPAE. In our study, the same analytical method with minor changes including the high energy in MS^E mode and MS/MS mode, was used to analyze the *in-vitro* and *in-vivo* samples. The pharmacokinetic parameters of RPAE have been investigated [17], but the studies on metabolism of RPAE are limited. There have been some reports on the metabolism studies of the components of RPAE, such as paeoniflorin, one main component of RPAE. Paeoniflorin possesses wide pharmacological effects in the nervous system. It has been used in the treatment of epilepsy, cerebral ischemia and neurodegenerative disorders such as Alzheimer's disease. And it also exhibits anticoagulant, neuromuscular blocking, cognition-enhancing and immunoregulating and antihyperglycemic effects. In Su et al.'s [18] study, metabolite hydroxyl-paeoniflorin was identified in rat plasma after oral administration of Shaofu Zhuyu decoction active extract. Previous studies had reported low bioavailability of orally administered paeoniflorin in rats (approximately 3–4%) [19,20], metabolism of paeoniflorin is an important mechanism that is responsible for poor bioavailability of paeoniflorin. Administered paeoniflorin was extensively metabolized into paeoniflorgenin, paeonimetabolins I and II [21–23]. Most of the components in RPAE possess the same parent structure and just differ in substituents such as thionyl, hydroxy and methyl. Besides, the content of paeoniflorin is larger compared to other monoterpene glycosides in RPAE and the reference of paeoniflorin could be purchased. Therefore, paeoniflorin is chosen as the representative to study the metabolism behaviors of monoterpene glycosides in RPAE. In our study, pure paeoniflorin was administered to rats to characterize the metabolic pathways of monoterpene glucosides. The results elucidate the analysis of the various metabolites of other monoterpene glucosides from RPAE.

In order to get more metabolism information of RPAE from the complex biological matrics, it is necessary to develop effective and reliable analytical methods for detection. Recently, UPLC–ESI-Q-TOF/MS system with automated MS^E data analysis software (Metabolynx™) has been proved to be a powerful and reliable analytical approach for *in vivo* metabolite identification studies [24–26]. With this efficient tool, we studied thoroughly the absorbed components and metabolites in rat bile, plasma and urine after oral administration of RPAE. These absorbed components and metabolites might be the bioactive substances of RPAE *in vivo* and should be screened on pharmacological models to pave a way for research on the effect related to the mechanism of action.

2. Materials and methods

2.1. Chemicals and regents

The standards of albiflorin, paeoniflorin and catechin (purity >98%, see their structures in Fig. 1) were purchased from the National Institute for Drug Control of China (Beijing, China). Acetonitrile (Merk, Germany), methanol (Merk, Germany) and formic acid (Fisher Scientific, Farilawn, NJ, USA) were of HPLC

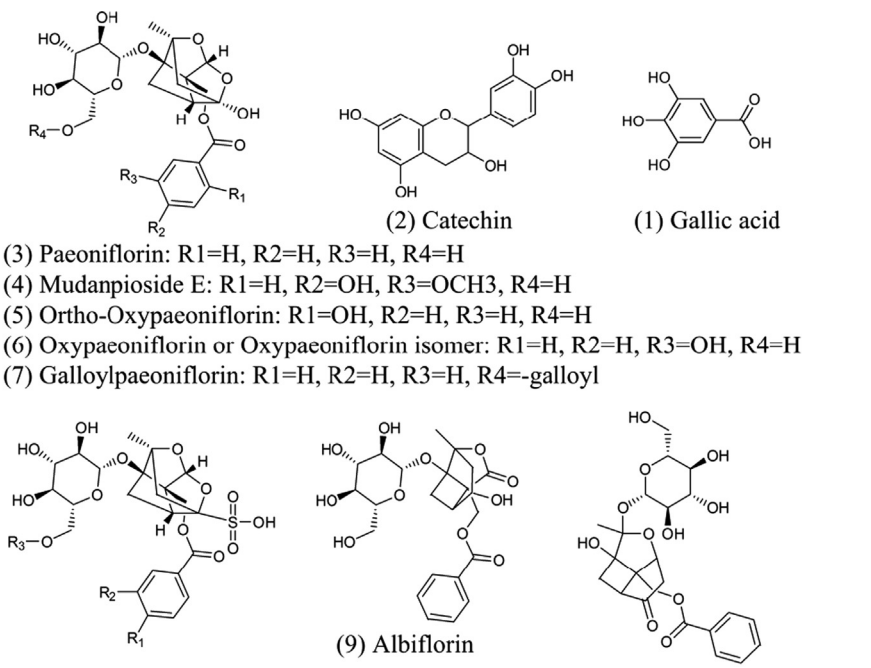

Fig. 1 Chemical structures of 14 parent compounds of RPAE.

grade, and other chemicals and regents were of analytical grade. De-ionized water was prepared by a Milli-Q purification system (Millipore, Bedford, MA, USA). Waters Oasis HLB Solid-phase extraction cartridge (30 mg/mL) was purchased from Waters Corp.

2.2. Preparation of RPAE

The dried powder of *Radix Paeoniae Alba* (Bozhou, Anhui, China) extract was supplied by Tianjin Tasly Pharmaceutical Co. Ltd (Tianjin, China). The preparation process was as follows: the pulverized samples of *Radix Paeoniae Alba* (50.0 g) was immersed in 400 mL water and extracted in a reflux water bath for 2 times, 2 h for each time. Proper amount of 95% ethanol was added into the extracts to adjust the concentration of ethanol to 70%. The solution was kept at 4 °C for 12 h then filtered. Cake was dried and went through 80 mesh sieve to yield RPAE. The RPAE was dissolved in methanol and filtered through a 0.22 μm membrane before analysis.

2.3. Animal experiments

Animal studies were conducted according to the protocols approved by the Animal Ethics Committee of Tasly Group. Animal experiments adhered to the National Institutes of Health Guide for the Care and Use of Laboratory Animals. Twenty four male Wistar rats (weighing 200 ± 20 g) were purchased from Beijing Vital River Laboratories (Beijing, China) and kept under controlled environmental conditions (temperature 22 ± 2 °C; humidity $50 \pm 10\%$) with free access to the standard laboratory food and water. The animals were divided into four groups with 6 rats in each group. One group was used for collection of bile after oral administration of paeoniflorin at the dose of 400 mg/kg. The other three groups were used for collection of bile, urine and plasma samples after oral administration of RPAE at the dose of 3 g/kg RPAE (namely, 18.75 g/kg for crude drug) respectively. The dose of RPAE was picked according to the publications on the pharmacokinetic studies of RPAE.

The rats were fasted for 12 h with free access to water prior to the experiments. Blank bile, plasma and urine samples were collected before administration with drugs. The rats were anesthetized with 20% urethane (m/m) at the dose of 0.7 mL/100 g, then fixed on wooden plates. An abdominal incision was made and bile duct was cannulated with PE tubing for collection of bile samples continually for 12 h after administration. The blood samples (0.5 mL each time) were collected from ophthalmic veins of the rats by sterile capillary tube at 0.5, 1, 2, 4 and 6 h after administration. The blood samples were centrifuged at 3500 rpm for 10 min immediately to get plasma. Urine samples were collected continually for 12 h after administration. Meanwhile the rats were kept free access to water. All the samples were stored at −20 °C.

2.4. Preparation of urine, plasma and bile samples

A solid-phase extraction (SPE) method was used for plasma and urine pretreatment. Before applying to sample, a SPE cartridge was treated with 1 mL of water, 1 mL of methanol and 1 mL of water successively. An aliquot of 0.5 mL plasma and urine sample was vortexed, loaded, and allowed to flow through the SPE cartridge with pressure. The SPE cartridge was then washed with 1 mL of water and 2 mL of methanol successively. The methanol eluate was collected and evaporated under a stream of N_2 at room temperature. The dried sample was dissolved in 200 μL methanol for analysis. The bile samples were mixed with acetonitrile (1:1, v/v) and centrifuged at $12{,}000 \times g$ for 10 min. The supernatant was used for analysis.

2.5. UPLC–Q-TOF/MS analytical system

Chromatographic experiments were performed on Waters Acquity UPLC system (Waters Corp., Milford, MA, USA) equipped with a 2998 photodiode array detector (PDA) together with a quaternary pump, an auto-sample injector, an on-line degasser and an automatic thermostatic column oven. The *in-vitro* and *in-vivo* samples were separated on a Waters Acquity UPLC HSS T3 column (2.1 mm × 100 mm; 1.8 μm) with the column temperature maintained at 35 °C. A linear gradient elution of solvent acetonitrile (A) and 0.1% formic acid aqueous solution (B, v/v) was applied with the following program: 2–5% A (0–2 min), 5–12% A (2–4 min), 12–20% A (4–8 min), 20–30% A (8–9 min), 30–50% A (9–10 min), and 50–100% A (10–12 min) at 0.3 mL/min. UV spectra were recorded from 190 to 400 nm. The temperature of autosampler tray was maintained at 4 °C through the analysis process. The injection volume was 2 μL for *in-vitro* samples and 10 μL for *in-vivo* samples.

The MS instrument consisted of a Waters Synapt G2 Q-TOF/MS (Waters Corp., Milford, MA, USA) equipped with an electrospray ionization (ESI) source. Both positive and negative ion modes were tested, and it was found that the sensitivities for most components in RPAE were higher in the negative ion mode. Ultrahigh purity argon (Ar) was used as the collision gas and high purity nitrogen (N_2) as the nebulizing gas. The nebulization gas was set to 650 L/h desolvation temperature at 300 °C, while the cone gas and the source temperature were set to 50 L/h and 90 °C, respectively. The capillary voltage and sample cone voltage were set to 2700 V and 35 V, respectively. The Q-TOF Premier acquisition rate was set to 0.3 s, with a 0.05 s inter-scan delay. Argon was employed as the collision gas at a pressure of 7.1×10^{-3} Pa. The energies for collision-induced dissociation (CID) were set at 5 eV in low energy and 30–50 eV ramp voltage in high energy in MS^E mode respectively for fragmentation information. For some peaks, the MS/MS mode at 30–50 eV ramp voltage was further employed to get the fragmentation information. All MS data were acquired using the LockSpray to ensure mass accuracy and reproducibility. The $[M-H]^-$ ion of leucine-enkephalin at m/z 554.2615 was used as the lock mass in negative electrospray ionization mode. The concentration of leucine-enkephalin was 2 ng/μL and the infusion flow rate was 5 μL/min. Sodium formate solution at the concentration of 0.5 mM was used to create the calibration file. The data were acquired in centroid mode with the mass ranged from 100 to 1000 Da. The Elemental Composition function of the software Metabolynx™ was used to predict the formulas of chemicals. Screening and identification of the metabolites of PRAE was assisted by the software Metabolynx™ (Waters Corp., Milford, MA, USA).

2.6. Software to calculate n-octanol/water partition coefficient (log P)

Software chembiodraw ultra 11.0 (Cambridgesoft®, Cambridge, MA) based on theoretical calculations was used to predict n-octanol/water partition coefficient (log *P*). The prediction of log *P* is based on 222 atomic contributions calculated from 1868 molecules by least squares analysis. This method allows a calculation of log *P* with a standard deviation of 0.43 log *P* units and can handle molecules containing hydrogen, oxygen, nitrogen, sulfur, halogens and phosphorus atoms.

Table 1 The compounds identified from bile, plasma and urine after oral administration of the RPAE by UPLC–ESI-Q-TOF/MS.

No.	RT (min)	*m/z* $[M–H]^-$ Found	PPM	Metabolite name	Formula $[M–H]^-$	Fragment ions	Parent drug	Identification	Bile	Plasma	Urine
M1	1.02	802.2350	1.1	+GSH+O	$C_{33}H_{45}N_3O_{18}S$	784,766,511,306,272,254,210,143,128	PAE		+	–	–
M2	1.03	453.0736	7.2	Hy–Glc+Glu	$C_{16}H_{22}O_{13}S$	179,277,	OPS		+	–	–
M3	1.04	262.9858	−1.5	$+CH_2+SO_3$	$C_8H_8O_8S$	183,168,150,124,203,96	GaA	3-Hydroxy-5-methoxy-4-(sulfooxy)benzoic acid	+	–	–
M4	1.05	671.1819	−0.7	+O+Glu	$C_{29}H_{36}O_{18}$	495,465,447,333,137	PAE		+	+	–
M5	1.06	575.1063	−1.4	$+O+SO_3$	$C_{23}H_{28}O_{15}S$		PAE		+	+	–
M6	3.09	262.9839	−8.7	$+CH_2+SO_3$	$C_8H_8O_8S$	183,168,150,124,203,96	GaA	3-Hydroxy-4-methoxy-5-(sulfooxy)benzoic acid	+	–	–
P1	3.15	359.1335	−1.9	–	$C_{16}H_{23}O_9$	179,197	–	1-O-β-D-Glucopyranosyl-paeonisuffrone	–	+	+
M7	3.51	453.0682	−4.7	Hy–Glc+Glu	$C_{16}H_{22}O_{13}S$	179,277,	OPS		+	–	–
M8	3.64	359.0607	−2.1	$+CH_2$+Glu	$C_{14}H_{16}O_{11}$	183,168,125,227,314,175,193	GaA		+	–	–
M9	3.74	345.0434	−7	+Glu	$C_{13}H_{14}O_{11}$	169,125,	GaA		+	–	–
M10	3.91	373.0779	2.1	$+2\times CH_2$+Glu	$C_{15}H_{18}O_{11}$	197,182,175,167,178,354,305	GaA		+	–	–
M11	3.97	671.1837	2	+O+Glu	$C_{29}H_{36}O_{18}$	495,465,375,345,281,195,177,152,137	IsP		+	–	–
M12	4.05	802.2358	2.1	+GSH+O	$C_{33}H_{45}N_3O_{18}S$	784,766,511,306,272,254,210,143,128	PAE		+	–	–
M13	4.16	233.0131	4.7	$+2\times CH_2–CO_2+SO_3$	$C_8H_{10}O_6S$	109,124,153	GaA	2,6-Dimethoxyphenyl hydrogen sulfate	+	–	–
M14	4.18	495.1513	2.1	+O	$C_{23}H_{28}O_{12}$	137,165,177,195,281, 283, 327,345,	PAE		+	+	–
P2	4.2	559.1122	0	–	$C_{23}H_{28}O_{14}S$	137,161,247,259,421	–	Oxypaeoniflorin sulfonate	+	+	+
M15	4.25	671.1831	1.1	+O+Glu	$C_{29}H_{36}O_{18}$	495,465,447,333,137	PAE		+	+	–
M16	4.31	802.2358	2.1	+GSH+O	$C_{33}H_{45}N_3O_{18}S$	784,766,511,306,272,254,210,143,128	PAE		+	–	–
M17	4.37	701.1921	−1.2	+Glu	$C_{30}H_{38}O_{19}$	363,453,525	ME		+	–	–
M18	4.4	262.9850	−4.5	$+CH_2+SO_3$	$C_8H_8O_8S$	183,168,150,124,203,96	GaA	4-Hydroxy-3-methoxy-5-(sulfooxy)benzoic acid	+	–	+
M19	4.43	717.1884	0.8	+O+Glu	$C_{30}H_{38}O_{20}$	225,255,312,327,461,651,669,687,493,543	ME		+	–	–
M20	4.5	373.0770	−0.3	$+2\times CH_2$+Glu	$C_{15}H_{18}O_{11}$	197,182,175,167,153	GaA		+	–	–
M21	4.61	701.1934	0.7	+Glu	$C_{30}H_{38}O_{19}$	239,327,363,495,525	ME		+	–	–
P3	4.68	589.1221	−1.1	–	$C_{24}H_{30}O_{15}S$	167,259,331,375,421,535,574	–	Isomaltopaeoniflorin sulfonate	+	+	+
M22	4.74	277.0017	−0.5	$+2\times CH_2+SO_3$	$C_9H_{10}O_8S$	107,124,167,182,197	GaA	3,5-Dimethoxy-4-(sulfooxy)benzoic acid	+	–	–
M23	4.88	621.1166	6.5	$+O+SO_3$	$C_{24}H_{30}O_{17}S$	225,327,346,361,445,511,541	ME		+	–	–
M24	4.91	495.1498	−1	+O	$C_{23}H_{28}O_{12}$	137,165,177,195,281, 283, 327,345,	PAE		+	+	–
M25	5	655.1887	1.9	+Glu	$C_{29}H_{36}O_{17}$	319,481	IsP		+	–	–
M26	5.01	605.1142	−5.7	+O	$C_{24}H_{30}O_{16}S$	183,241,525,544	MES	6-Hydroxy mudanpioside E sulfonate	+	–	–
M27	5.01	701.1924	−0.8	+Glu	$C_{30}H_{38}O_{19}$	285,525	ME		+	–	–
M28	5.02	575.1044	−4.7	$+O+SO_3$	$C_{23}H_{28}O_{15}S$	137,495,465	PAE		+	+	–
M29	5.04	717.1868	−1.5	+O+Glu	$C_{30}H_{38}O_{20}$	284,511,543,574	ME		+	+	–
P4	5.16	705.1695	−0.8	–	$C_{29}H_{38}O_{18}S$	121,259,421,543,583	–	Mudanpioside E sulfonate	+	+	+
M30	5.28	575.1054	−2.9	$+O+SO_3$	$C_{23}H_{28}O_{15}S$	137,495,465	PAE		+	+	–
M31	5.3	605.1144	−5.4	+O	$C_{24}H_{30}O_{16}S$	183,495,525	MES	2-Hydroxy mudanpioside E sulfonate	+	–	–
P5	5.32	543.117	−0.5	–	$C_{23}H_{28}O_{13}S$	121,213,259,375,421	–	Paeoniflorin sulfonate	+	+	+
M32	5.32	479.1189	−0.2	$+CH_2$+Glu	$C_{22}H_{24}O_{12}$	202,217,244,259,285,303	Cat		+	+	–
M33	5.38	717.1868	−1.5	+O+Glu	$C_{30}H_{38}O_{20}$		ME		+	+	–
M34	5.43	605.1143	−5.5	+O	$C_{24}H_{30}O_{16}S$	183,277,403,425,439,525,	MES	5-Hydroxy mudanpioside E sulfonate	+	–	–
M35	5.54	479.1190	0	$+CH_2$+Glu	$C_{22}H_{24}O_{12}$	219,244,259,285,303	Cat		+	+	–
M36	5.55	383.0439	0.5	$+CH_2+SO_3$	$C_{16}H_{16}O_9S$	303,285,259,244,216,202,164,137	Cat		+	+	–
M37	5.55	621.1121	−0.8	$+O+SO_3$	$C_{24}H_{30}O_{17}S$	210,255,285,327,346,361,445,493,407,541	ME		+	–	–
M38	5.63	449.1465	3.8	$–CH_2–O$	$C_{22}H_{26}O_{10}$	165,327,273,309,291,386,430,447	IsP		+	–	–

Table 1 (*continued*)

No.	RT (min)	*m/z* [M–H]$^-$ Found	PPM	Metabolite name	Formula [M–H]$^-$	Fragment ions	Parent drug	Identification	Bile	Plasma	Urine
M39	5.65	373.0757	−3.8	+2 × CH_2+Glu	$C_{15}H_{18}O_{11}$	197,182,193,167,175,250,255	GaA		+	−	−
M40	5.66	479.1203	2.8	+CH_2	$C_{22}H_{24}O_{12}$	219,244,259,285,303	Cat		+	+	−
M41	5.67	701.1915	−2	+Glu	$C_{30}H_{38}O_{19}$	363,525	ME		+	−	−
P6	5.79	495.1488	−3	–	$C_{23}H_{28}O_{12}$	137,165,289, 407,421,465	–	Oxypaeoniflorin or oxypaeoniflorin isomer	+	−	−
M42	6.13	277.0023	1.7	+2 × CH_2+SO_3	$C_9H_{10}O_8S$	107,124,167,182,197	GaA	3,4-Dimethoxy-5-(sulfooxy)benzoic acid	+	−	−
M43	6.34	495.1483	−4	+O	$C_{23}H_{28}O_{12}$	137,165, 283, 327,345,	PAE		+	−	+
M44	6.37	621.1127	0.2	+O+SO_3	$C_{24}H_{30}O_{17}S$	345,427,445,523,541,	ME		+	−	
M45	6.47	479.1191	0.3	+CH_2+Glu	$C_{22}H_{24}O_{12}$	219,244,259,285,303	Cat		+	−	+
M46	6.6	621.1140	2.3	+O+SO_3	$C_{24}H_{30}O_{17}S$	511,523,541	ME		+	−	−
M47	6.72	233.0103	−7.3	+2 × CH_2–CO_2+SO_3	$C_8H_{10}O_6S$	109,124,153	GaA	2,3-Dimethoxyphenyl hydrogen sulfate	+	−	−
M48	6.86	383.0431	−1.6	+CH_2+SO_3	$C_{16}H_{16}O_9S$	303,285,259,244,216,202,164,137	Cat		+	−	−
M49	6.96	655.1865	−1.4	+Glu	$C_{29}H_{36}O_{17}$	319,481	IsP		+	−	−
M50	7.14	449.1446	−0.4	–CH_2–O	$C_{22}H_{26}O_{10}$	165,327,273,309,291,386,430,447	IsP		+	+	−
M51	7.29	577.1219	−1.5	+H_2+O	$C_{23}H_{30}O_{15}S$	272,382,400,497	OPS		+	−	−
P7	7.33	479.1562	1.7	–	$C_{23}H_{28}O_{11}$	121,195,283, 327,357,375	–	Albiflorin	+	+	+
M52	7.49	383.0431	−1.6	+CH_2+SO_3	$C_{16}H_{16}O_9S$	303,285,259,244,216,202,164,137	Cat		+	+	−
M53	7.7	655.1886	1.8	+Glu	$C_{29}H_{36}O_{17}$	319,481	IsP		+	−	−
M54	7.79	449.1444	−0.9	–CH_2–O	$C_{22}H_{26}O_{10}$	165,327,273,309,291,386,430,447	IsP		+	+	+
P8	7.81	479.1543	−2.2	–	$C_{23}H_{28}O_{11}$	121,165,283, 327,345,431,449	–	Paeoniflorin	+	+	+
P9	8.25	495.1502	−0.2	–	$C_{23}H_{28}O_{12}$	137,169,325,443	–	Ortho-oxypaeoniflorin	+	−	−
P10	9.46	631.1661	−0.3	–	$C_{30}H_{32}O_{15}$	169,313,399,	–	Galloylpaeoniflorin or galloylalbiflroin or their isomers	+	−	−
P11	10.24	647.1447	1.9	–	$C_{30}H_{32}O_{14}S$	121,169,213,259,313,479,525,631	–	Benzoylpaeoniflorin sulfonate	+	+	+

1. Cat: catechin; GaA: gallic acid; IsP: isomer of paeoniflorin; ME: Mudanpioside E; MES: Mudanpioside E sulfonate; OPS: Oxypaeoniflorin sulfonate; PAE: paeoniflorin.
2. –CO_2: Decarboxylation; +SO_3: sulfate conjugation; +Glu: glucuronide conjugation; –CH_2: demethylation; +CH_2: methylation; –O: loss of oxygen; +O: hydroxylation; +GSH: glutathione conjugation; Hy: hydrolisis; –Glc: deglucose; +H_2: reduction.
3. P: the parent components in RPAE; M: metabolites; PPM: parts per million.
4. +: detected, −: not detected.

If this method is applied to molecules with internal hydrogen bonds, the standard deviation is 0.83 log *P* units.

3. Results and discussion

3.1. Identification of components from RPAE in vitro

RPAE was dissolved in methanol and filtered through a 0.22 μm membrane filter unit, and 2 μL was injected for analysis. Compounds albiflorin, paeoniflorin and catechin in RSE were unambiguously identified by the comparison of retention time (t_R), UV spectrum, and fragments information as shown in Table 1 with their standards. The rest peaks in the chromatograms of RPAE were identified by comparing their accurate masses, retention time, UV spectra and fragmentation information with those reported in literature [12–16]. Chemical structures of 14 parent compounds of RPAE are shown in Fig. 1.

3.2. Identification of parent components in bile, plasma and urine after oral administration of RPAE

By comparing the accurate masses, retention time and fragmentation information of peaks appearing in the chromatograms of bile, plasma and urine with those previously identified in RPAE *in vitro*, 11 peaks were detected as prototype components of RPAE. Their extracted ion chromatograms are shown in Fig. 2.

3.3. Characterization of metabolites of single standard

RPAE contains multiple compounds with significant varieties in structural types, physiochemical properties, and relative amounts. When they were administered by oral route, lots of compounds may get into circulation and then be converted into a mixture of metabolites of unknown origin. Meanwhile, chemicals in herbal medicine usually present in the form of a series of analogs with the same skeleton but different functionalities and their metabolites may undergo similar fragmentation and produce some of the same ions. Understanding the metabolic pathway of certain parent drugs will greatly facilitate metabolite identification of their analogs. Therefore, in our study paeoniflorin was chosen as the representative to study the metabolic pathways of monoterpene glycosides. The fragmentation pathways of paeoniflorin (shown in Fig. 3) were investigated thoroughly which will throw light upon the identification of the metabolites. In addition, as only one single compound was fed to rats, the metabolic profiles were easy to be elucidated. The result indicated that hydroxylation, glucuronidation, glutathione (GSH) conjugation and sulfation predominated the metabolism of paeoniflorin.

3.4. n-octanol/water partition coefficient (log P)

It was common that several metabolites were assigned as isomers in biological matrices. To elucidate the exact structures of these isomers, such as the positions of conjugation or hydroxylation, were challenging due to little differences present in their MS spectra. Log *P*, an important parameter in the process of designing new drugs, provides the direct information on hydrophobicity that describes the tendency of distribution of a drug from aqueous phase into biological membranes [27]. Software chembiodraw ultra 11.0 was used to predict Log *P*. Generally, for compounds with log $P<4$, the calculated log *P* values are almost the same as the experimental measurements. The larger log *P* is the less retention time it would have on the reverse phase chromatography [28,29].

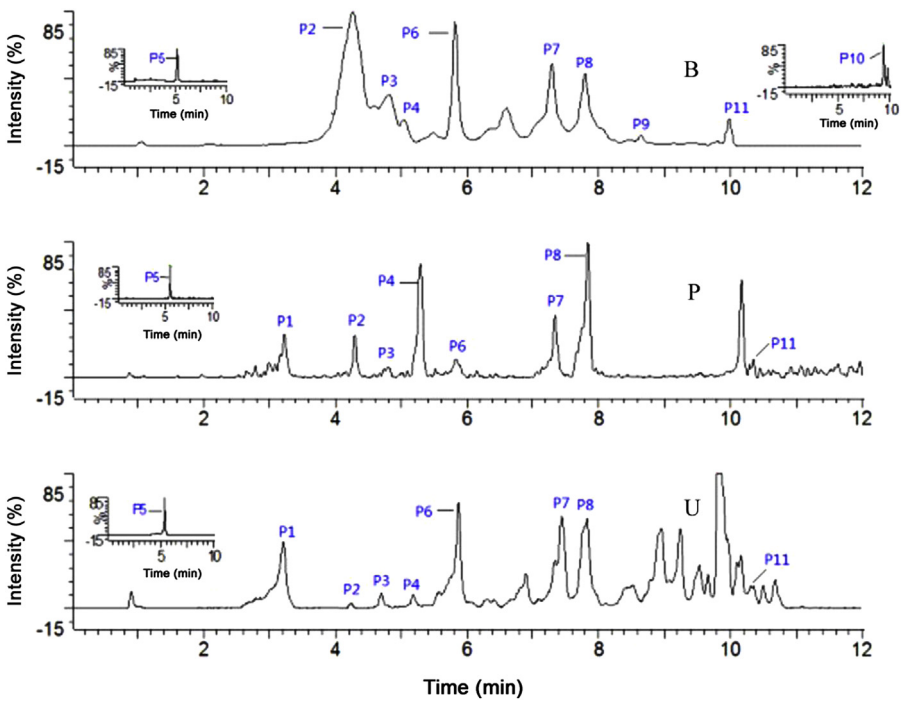

Fig. 2 Extracted ion chromatograms in negative mode of 11 parent compounds (P1–P11) detected in bile (B), plasma (P) and urine (U). P1–P11 are 1-O-β-D-glucopyranosyl-paeonisuffrone, oxypaeoniflorin sulfonate, isomaltopaeoniflorin sulfonate, mudanpioside E sulfonate, paeoniflorin sulfonate, oxypaeoniflorin or oxypaeoniflorin isomer, albiflorin, paeoniflorin, ortho-oxypaeoniflorin, galloylpaeoniflorin or galloylalbiflroin or their isomers, benzoylpaeoniflorin sulfonate, respectively.

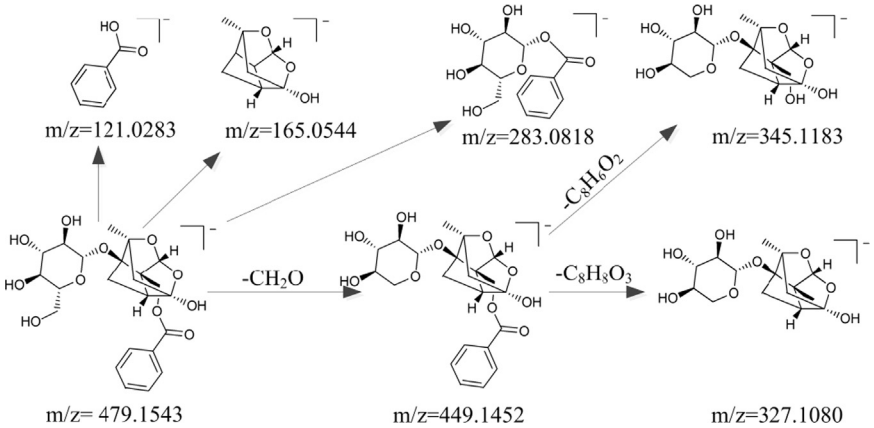

Fig. 3 Proposed fragmentation pathways of paeoniflorin.

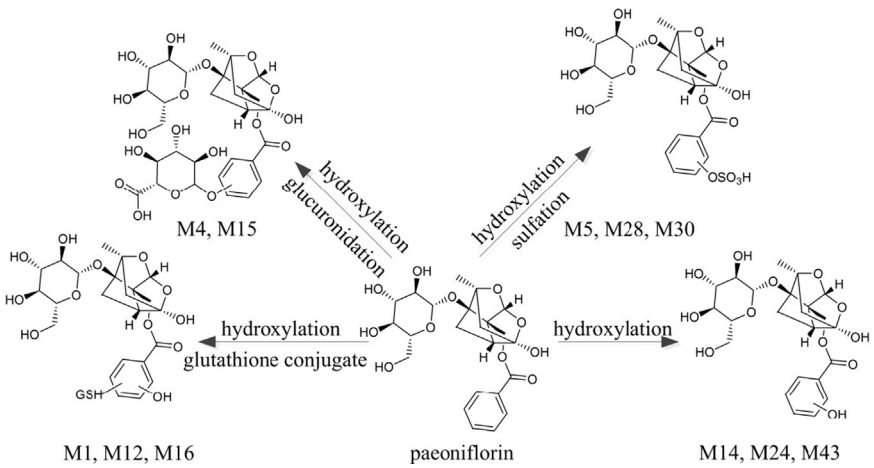

Fig. 4 Proposed metabolic pathways of paeoniflorin-related metabolites.

3.5. Identification of metabolites from bile, urine, plasma after oral administration of RPAE

Besides the 11 prototype compounds, 54 peaks were tentatively presumed to be metabolites of RPAE, and could be generally divided into three groups: monoterpene glycosides-related, catechin-related and gallic acid-related metabolites.

3.5.1. Identification of monoterpene glycoside-related metabolites

3.5.1.1. Identification of paeoniflorin-related metabolites. A total of 11 compounds detected in rat bile, plasma and urine were tentatively assigned as metabolites originating from paeoniflorin. From the results shown in Table 1, we can see that paeoniflorin underwent hydroxylation before undergoing phase II metabolic reaction. They all shared the same fragment ion at *m/z* 137 corresponding to the hydroxylated benzene ring.

M14, M24 and M43 shared a series of characteristic ions at *m/z* 165, 283, 327 and 345 with paeoniflorin. In addition, according to the accurate molecular mass, M14, M24 and M43 were 16 Da higher than paeoniflorin. Thus, M14, M24 and M43 were assigned as hydroxylation products of paeoniflorin. The shorter retention time of M14, M24 and M43 than that of paeoniflorin (t_R = 7.81 min) on the RP-UPLC column also supported the tentative identification as oxidation metabolites of paeoniflorin.

M5, M28 and M30 shared a series of characteristic ions of hydroxylated paeoniflorin at *m/z* 495, 465 and 137. In addition, the molecular weight of M5, M28 and M30 was 80 Da (SO_3) higher than that of hydroxylated paeoniflorin, indicating that they were sulfate conjugates of hydroxylated paeoniflorin. M4 and M15 shared a series of characteristic ions of hydroxylated paeoniflorin at *m/z* 447 and 333. The molecular weight of M4 and M15 was 176 Da higher than that of hydroxylated paeoniflorin, indicating that they were glucuronide conjugates of hydroxylated paeoniflorin.

For metabolites M1, M12 and M16, a series of characteristic ions of glutathione at *m/z* 306, 272, 254, 210, 143 and 128 were observed. Their molecular weight was 307 Da higher than hydroxylated paeoniflorin, so they were tentatively identified as glutathione conjugates of hydroxylated paeoniflorin. The proposed metabolic pathways of paeoniflorin are shown in Fig. 4 and the extracted ion chromatograms of paeoniflorin-related metabolites are shown in Fig. 5.

3.5.1.2. Identification of mudanpioside E-related metabolites. Metabolites M23, M37, M44 and M46 gave $[M-H]^-$ ions at *m/z* 621.1166, 621.1121, 621.1127 and 621.1140 respectively, which were calculated as $C_{30}H_{38}O_{19}$ by the Elemental Composition function of software Metabolynx™. Their different retention times suggested they were isomers. They shared a series of characteristic ions at *m/z* 345, 511, 523 and 541 with mudanpioside E. The $[M-H]^-$ ion at *m/z* 621 yielded a product ion at *m/z* 541 with a loss of 80 Da (SO_3), suggesting that they were

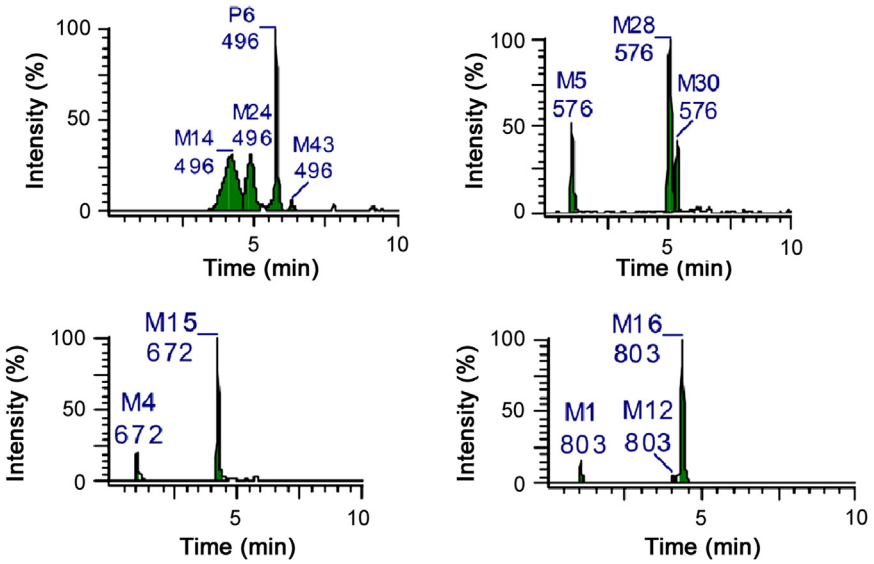

Fig. 5 Extracted ion chromatograms of paeoniflorin-related metabolites from rat bile in negative mode.

sulfate conjugates. In addition, the ion at *m/z* 541 is 16 Da higher than that of mudanpioside E, indicating that M23, M37, M44 and M46 were sulfate conjugates of hydroxylated mudanpioside E.

According to the accurate mass, the molecular weight of M17, M21, M27 and M41 was 176 Da higher than that of mudanpioside E. In addition, their fragments ions were similar to that of mudanpioside E, suggesting that they were glucuronide conjugates of mudanpioside E. While the molecular weight of M19, M29 and M33 was 16 Da higher than that of M17, suggesting that they were glucuronide conjugates of hydroxylated mudanpioside E. The proposed metabolic pathways of mudanpioside E are shown in Fig. 6 and the extracted ion chromatograms of mudanpioside E-related metabolites are shown in Fig. 7.

3.5.1.3. Identification of mudanpioside E sulfate-related metabolites. M26, M31 and M34 yielded an ion at *m/z* 183, indicating that the benzene ring was hydroxylated. In addition, their $[M-H]^-$ ion at *m/z* 605 gave a product ion at *m/z* 525 with a loss of 80 Da (SO_3) and their molecular weight was 16 Da higher than that of mudanpioside E sulfate, so they were tentatively identified as hydroxylated mudanpioside E sulfate. There were three places in the benzene ring of mudanpioside E sulfate that could be hydroxylated. According to the fact that one with a larger log *P* value would have less retention time on the reverse phase chromatography, M26 (t_R = 5.01 min, log *P* = −3.648), M31 (t_R = 5.3 min, log *P* = –3.898) and M34 (t_R = 5.43 min, log *P* = –3.928) were tentatively identified as 6-hydroxy mudanpioside E sulfonate, 2-hydroxy mudanpioside E sulfonate and 5-hydroxy mudanpioside E sulfonate, respectively. The extracted ion chromatograms of mudanpioside E-related metabolites are shown in Fig. 7.

3.5.1.4. Identification of oxypaeoniflorin sulfonate-related metabolites. Metabolites M2 and M7 gave a $[M-H]^-$ ion at *m/z* 453.0682 and 453.0736 respectively, calculated as $C_{16}H_{22}O_{13}S$. In addition, M2 and M7 gave an ion at *m/z* 277 with a loss of 176 Da, suggesting that they were glucuronide conjugates. Based on the information above, M2 and M7 were tentatively identified as glucuronide conjugates after oxypaeoniflorin sulfonate undergoing hydrolysis and deglucose reactions. M51 gave a $[M-H]^-$ ion at *m/z* 577.1219 ($C_{23}H_{30}O_{15}S$), which yielded a product ion at *m/z* 497 with a loss of 80 Da (SO_3), corresponding to the characteristic loss of oxypaeoniflorin sulfonate. Thus M51 was tentatively identified as the reduction and hydroxylation product of oxypaeoniflorin sulfonate. The extracted ion chromatograms of oxypaeoniflorin sulfonate-related metabolites are shown in Fig. 8.

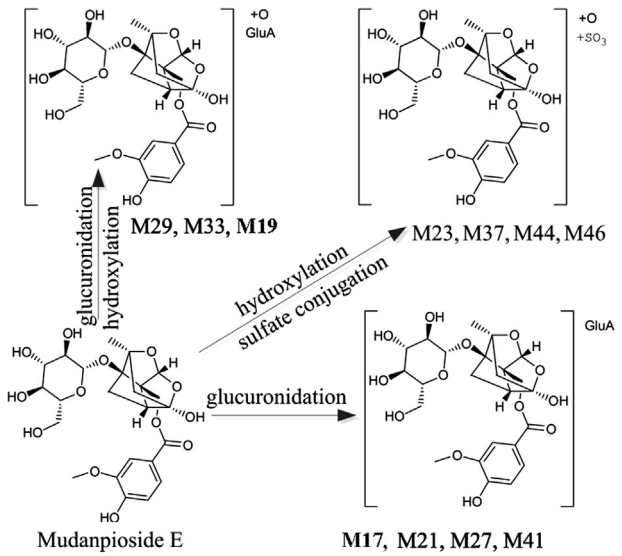

Fig. 6 Proposed metabolic pathways of mudanpioside E-related metabolites.

3.5.1.5. Identification of isomer of paeoniflorin-related metabolites. Three isomers of paeoniflorin (*m/z* = 479.1543, $C_{23}H_{28}O_{11}$) were identified *in vitro* as albiflorin, isopaeoniflorin and albiflorin R1 according to their fragmentation information. M25, M49 and M53 produced fragment ions at *m/z* 319 and 481, corresponding to loss of 176 Da and 162 Da. So they were tentatively identified as glucuronide conjugates of isomer of paeoniflorin. The molecular weight of M11 was 16 Da (O) higher than that of M25 and also shared the loss of 176 Da. Thus M11 was tentatively identified as glucuronide conjugate of hydroxylated isomer of paeoniflorin. M38, M50 and M54 gave $[M-H]^-$ ions at *m/z* 449.1465,

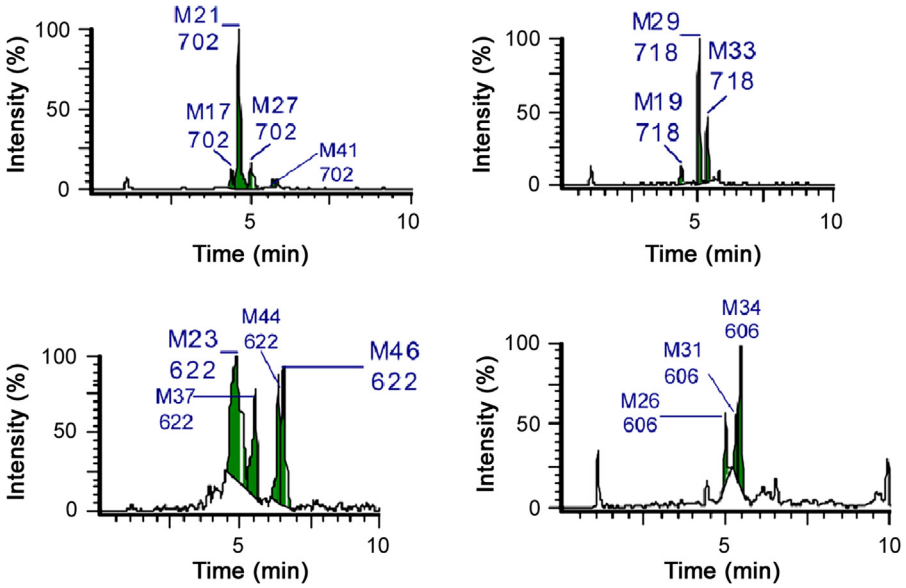

Fig. 7 Extracted ion chromatograms of mudanpioside E-related and mudanpioside E sulfate-related metabolites from rat bile in negative mode.

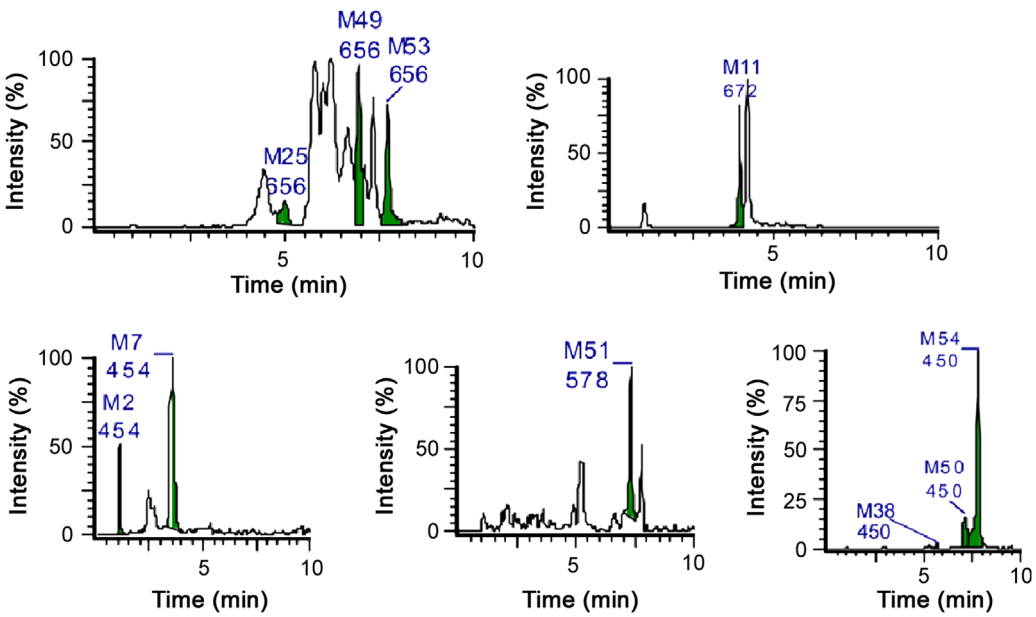

Fig. 8 Extracted ion chromatograms of oxypaeoniflorin sulfate and isomer of paeoniflorin-related metabolites from rat bile in negative mode.

449.1446 and 449.1444 respectively, which were calculated as $C_{22}H_{26}O_{10}$. They shared the same characteristic ions at *m/z* 165 and 327 with paeoniflorin. Moreover, compared with the molecular weight of paeoniflorin, they were 30 Da less, which was tentatively assigned to CH_2 (14 Da) and O (16 Da). Thus M38, M50 and M54 were tentatively identified as demethylation and loss of oxygen products of isomer of paeoniflorin. The extracted ion chromatograms of isomer of paeoniflorin-related metabolites are shown in Fig. 8.

3.5.2. Identification of catechin-related metabolites

M36, M48 and M52 gave $[M-H]^-$ ions at *m/z* 383, which produced a product ion at *m/z* 303 with a loss of 80 Da (SO_3), indicating that they were sulfate conjugates. The presence of ions at *m/z* 259 and 244 suggested that there was a methyl group (15 Da). Thus M36, M48 and M52 were tentatively identified as methylation and sulfation conjugates of catechin. M32, M35, M40 and M45 gave a $[M-H]^-$ ion at *m/z* 479, which produced a product ion at *m/z* 303 with a loss of 176 Da, indicating that they were glucuronide conjugates. The presence of product ions at *m/z* 259 and 244 suggested that there was a methyl group (15 Da). Thus M32, M35, M40 and M45 were tentatively identified as methylation and glucuronide conjugates of catechin. The extracted ion chromatograms of catechin-related metabolites are shown in Fig. 9.

3.5.3. Identification of gallic acid-related metabolites

M22 and M42 gave a $[M-H]^-$ ion at *m/z* 277, which gave a product ion at *m/z* 197 with a loss of 80 Da (SO_3), suggesting that they were sulfate conjugates. The presence of product ions at

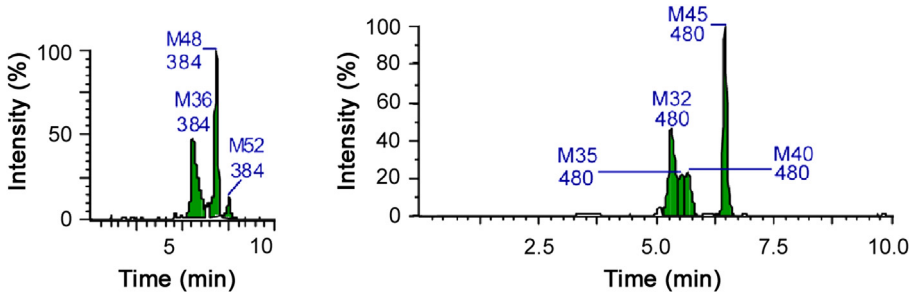

Fig. 9 Extracted ion chromatograms of catechin-related metabolites from rat bile in negative mode.

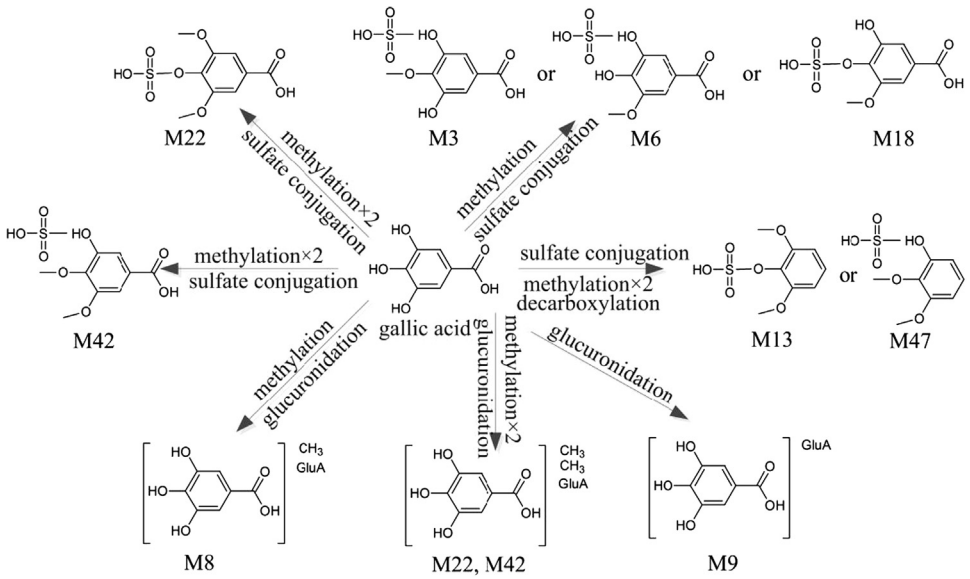

Fig. 10 Proposed metabolic pathways of gallic acid-related metabolites.

m/z 197,182 and 167 indicated that there were two methyl groups. So M22 and M42 were assigned as sulfation and double methylation conjugates of gallic acid. According to the fact that one with larger log *P* value would have less retention time on the reverse phase chromatography, M22 (t_R = 4.73 min, log *P* = –0.189) and M42 (t_R = 6.13 min, log *P* = –0.539) were tentatively identified as 3,5-dimethoxy-4-(sulfooxy)benzoic acid and 3,4-dimethoxy-5-(sulfooxy)benzoic acid, respectively.

As for M13 and M47, the $[M-H]^-$ ion at *m/z* 233.0131 ($C_8H_{10}O_6S$) was 44 Da less than that of M22, suggesting that they were the decarboxylation products of M22. Thus M13 and M47 were assigned as decarboxylation products after sulfation and double methylation of gallic acid. M13 (t_R = 4.16 min, log *P* = –0.004) and M47 (t_R = 6.72 min, log *P* = –0.354) were tentatively identified as 2,6-dimethoxyphenyl hydrogen sulfate and 2,3-dimethoxyphenyl hydrogen sulfate, respectively. M3, M6 and M18 gave a $[M-H]^-$ ion at *m/z* 263, which yielded product ions at *m/z* 183 and 168, with a loss of 80 Da (SO_3) and 15 Da (CH_3). Thus M3, M6 and M18 were assigned as methylation and sulfate conjugates of gallic acid.

M9 gave a $[M-H]^-$ ion at 345.0434 ($C_{13}H_{14}O_{11}$), which led to a product ion at *m/z* 169 with the loss of 176 Da, suggesting that it was glucuronide conjugate of gallic acid. The molecular weight of M8 was 14 Da (CH_2) higher than that of M9, indicating that M8 was methylated M9. So M8 was tentatively identified as methylation and glucuronide conjugate of gallic acid.

M10, M20 and M39 yielded $[M-H]^-$ ions at *m/z* 373, which could lead to fragment ion at *m/z* 197 with a loss of 176 Da, suggesting that they were glucuronide conjugates. Moreover, the presence of product ions at *m/z* 197, 182 and 167 implied that there were two methyl groups. Thus M10, M20 and M39 were tentatively identified as glucuronide and double methylation conjugates of gallic acid. The proposed metabolic pathways of gallic acid are shown in Fig. 10 and the extracted ion chromatograms of gallic acid-related metabolites are shown in Fig. 11.

3.6. *Discussions*

Isomers are the groups of compounds with the same exact masses and elemental compositions. In most cases, these compounds are similar in structure and polarity and also have similar cleavage pathways, which is difficult for analysts to deal with [30]. As for LC–MS method, there are three ways to distinguish them, including the retention time, the differences of fragment ions and UV spectra. For some isomers, they could be distinguished by analyzing their retention time and n-octanol/water partition coefficient. The larger the n-octanol/water partition coefficient is, the smaller the retention time is on the reverse phase chromatography. The software chembiodraw ultra 11.0 could be used to calculate the n-octanol/water partition coefficient. The maximum absorption wavelength in UV spectra will change according to the different positions of these moieties. So the UV spectra can help pinpoint

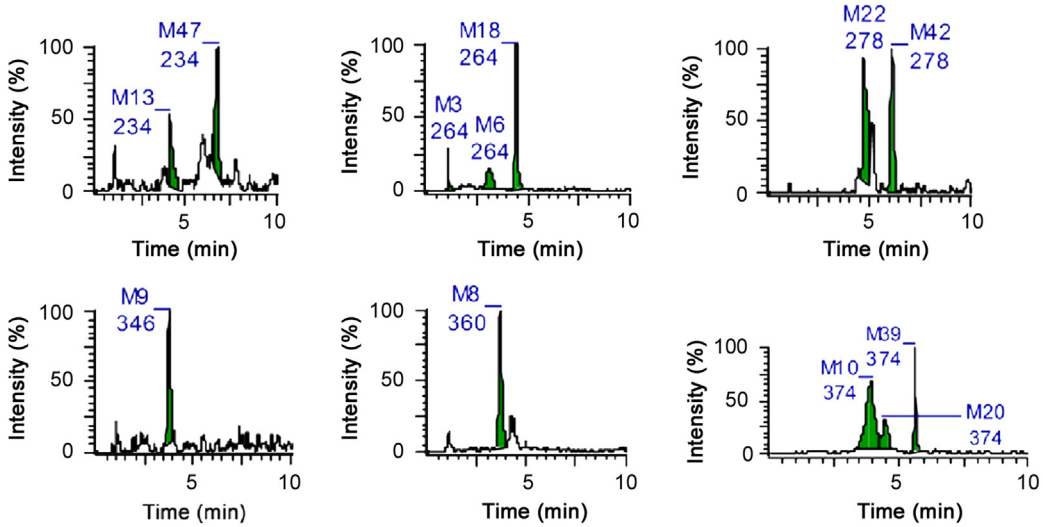

Fig. 11 Extracted ion chromatograms of gallic acid-related metabolites from rat bile in negative mode.

the position of conjugations. However, in our study, the polarities of the metabolites are very close that make it impossible to separate them completely on chromatography, so the UV spectra could not be used to distinguish them. For most of the isomers, the difference of fragmentation information could hardly be found as the structures seem so alike. Therefore, judging from the factors illustrated above, some metabolites in our study cannot be given exact structures. Further studies such as ^{1}H and ^{13}C NMR are needed to clarify the exact structures of these isomers.

4. Conclusion

In our study, a total of 54 metabolites were detected and the metabolic pathways were proposed. This is the first study to establish the metabolic profile of RPAE, which is helpful in revealing the bioactive components of RPAE. Moreover, it was demonstrated that the high-speed and sensitive UPLC–Q-TOF/MS analytical system combined with the software Metabolynx™ was a useful tool to identify metabolites in herbal medicine.

References

[1] X.Y. Gao, G.Y. Tian, Active principles of *Paeonia lactiflora* Pall, Zhongguo Xinyao Zazhi 6 (2006) 416–418.
[2] X.G. Weng, S.Q. Nie, L.Q. Huang, A survey of studies on paeoniaceae, Zhongguo Shiyan Fangjixue Zazhi 9 (2003) 55–59.
[3] X.Y. Zhang, X. Li, Development of the study on chemical constituents of *Paeonia lactiflora* Pall, Shenyang Yao Ke Da Xue Xue Bao 19 (2002) 70–73.
[4] Y. Chang, W. Wei, L. Zhang, et al., Effects and mechanisms of total glucosides of paeony on synoviocytes activities in rat collagen-induced arthritis, J. Ethnopharmacol. 121 (2009) 43–48.
[5] T. Okubo, F. Nagai, T. Seto, et al., The inhibition of phenylhydroquinone-induced oxidative DNA cleavage by constituents of Moutan cortex and Paeoniae radix, Biol. Pharm. Bull. 23 (2000) 199–203.
[6] B. Lee, Y.W. Shin, E.A. Bae, et al., Antiallergic effect of the root of *Paeonia lactiflora* and its constituents paeoniflorin and paeonol, Arch. Pharm. Res. 31 (2008) 445–450.
[7] J. Ye, H. Duan, X. Yang, et al., Anti-thrombosis effect of paeoniflorin: evaluated in a photochemical reaction thrombosis model *in vivo*, Planta Med. 67 (2001) 766–767.
[8] D.F. Liu, W. Wei, L.H. Song, Protective effect of paeoniflorin on immunological liver injury induced by bacillus calmette-guerin plus lipopolysaccharide: modulation of tumour necrosis factor-α and interleukin-6 mRNA, Clin. Exp. Pharmacol. Physiol. 33 (2006) 332–339.
[9] H. Ohta, J.W. Ni, K. Matsumoto, et al., Peony and its major constituent, paeoniflorin, improved radial maze performance impaired by scopolamine in rats, Pharmacol. Biochem. Behav. 45 (1993) 719–723.
[10] F.L. Hsu, C.W. Lai, J.T. Cheng, Antihyperglycemic effects of paeoniflorin and 8-debenzoylpaeoniflorin, glucosides from the root of *Paeonia lactiflora*, Planta Med. 63 (1997) 323–325.
[11] P. Zhang, J.J. Zhang, J. Su, et al., Effect of total glucosides of paeony on the expression of nephrin in the kidneys from diabetic rats, Am. J. Chin. Med. 37 (2010) 295–307.
[12] C. Han, Y. Shen, J. Chen, et al., HPLC fingerprinting and LC–TOF-MS analysis of the extract of *Pseudostellaria heterophylla* (Miq.) Pax root, J. Chromatogr. B Anal. Technol. Biomed. Life Sci. 862 (2008) 125–131.
[13] Y. Jiang, S.P. Li, Y.T. Wang, et al., Differentiation of Herba Cistanches by fingerprint with high-performance liquid chromatography–diode array detection-mass spectrometry, J. Chromatogr. A 1216 (2009) 2156–2162.
[14] J. Li, W.Z. Li, W. Huang, et al., Quality evaluation of Rhizoma Belamcandae (*Belamcanda chinensis* (L.) DC.) by using high-performance liquid chromatography coupled with diode array detector and mass spectrometry, J. Chromatogr. A. 1216 (2009) 2071–2078.
[15] W. Li, Y. Deng, R. Dai, et al., Chromatographic fingerprint analysis of *Cephalotaxus sinensis* from various sources by high-performance liquid chromatography–diodearray detection-electrospray ionization-tandem mass spectrometry, J. Pharm. Biomed. Anal. 45 (2007) 38–46.
[16] S.L. Li, J.Z. Song, F.F.K. Choi, et al., Chemical profiling of Radix Paeoniae evaluated by ultra-performance liquid chromatography/photo-diode-array/quadrupole time-of-flight mass spectrometry, J. Pharm. Biomed. Anal. 49 (2009) 253–266.
[17] C. Feng, M. Liu, X. Shi, et al., Pharmacokinetic properties of paeoniflorin, albiflorin and oxypaeoniflorin after oral gavage of extracts of Radix Paeoniae Rubra and Radix Paeoniae Alba in rats, J. Ethnopharmacol. 130 (2010) 407–413.
[18] S. Su, J. Guo, J. Duan, et al., Ultra-performance liquid chromatography–tandem mass spectrometry analysis of the bioactive components and their metabolites of Shaofu Zhuyu decoction active extract in rat plasma, J. Chromatogr. B Anal. Technol. Biomed. Life Sci. 878 (2010) 355–362.

[19] S. Takeda, T. Isono, Y. Wakui, et al., Absorption and excretion of paeoniflorin in rats, J. Pharm. Pharmacol. 47 (1995) 1036–1040.
[20] S. Takeda, T. Isono, Y. Wakui, et al., *In-vivo* assessment of extrahepatic metabolism of paeoniflorin in rats: relevance to intestinal floral metabolism, J. Pharm. Pharmacol. 49 (1997) 35–39.
[21] C. Wang, R. Wang, X. Cheng, et al., Comparative pharmacokinetic study of paeoniflorin after oral administration of decoction of Radix Paeoniae Rubra and Radix Paeoniae Alba in rats, J. Ethnopharmacol. 117 (2008) 467–472.
[22] S.L. Hsiu, Y.T. Lin, K.C. Wen, et al., A deglucosylated metabolite of paeoniflorin of the root of *Paeonia lactiflora* and its pharmacokinetics in rats, Planta Med. Nat. Prod. Med. Plant Res. 69 (2003) 1113–1118.
[23] M. Hattori, Y.Z. Shu, M. Shimizu, et al., Metabolism of paeoniflorin and related compounds by human intestinal bacteria, Chem. Pharm. Bull. (Tokyo) 33 (1985) 3838–3846.
[24] K.P. Bateman, J. Castro-Perez, M. Wrona, et al., MS^E with mass defect filtering for *in vitro* and *in vivo* metabolite identification, Rapid Commun. Mass Spectrom. 21 (2007) 1485–1496.
[25] J. Castro-Perez, R. Plumb, J.H. Granger, et al., Increasing throughput and information content for *in vitro* drug metabolism experiments using ultra-performance liquid chromatography coupled to a quadrupole time-of-flight mass spectrometer, Rapid Commun. Mass Spectrom. 19 (2005) 843–848.
[26] R.J. Mortishire-Smith, D. O'Connor, J.M. Castro-Perez, et al., Accelerated throughput metabolic route screening in early drug discovery using high-resolution liquid chromatography/quadrupole time-of-flight mass spectrometry and automated data analysis, Rapid Commun. Mass Spectrom. 19 (2005) 2659–2670.
[27] W.J. Lambert, Modeling oil–water partitioning and membrane permeation using reversed-phase chromatography, J. Chromatogr. A 656 (1993) 469–484.
[28] D.J. Minick, D.A. Brent, J. Frenz, Modeling octanol–water partition coefficients by reversed-phase liquid chromatography, J. Chromatogr. A. 461 (1989) 177–191.
[29] W. Zhang, M.W. Saif, G.E. Dutschman, et al., Identification of chemicals and their metabolites from PHY906, a Chinese medicine formulation, in the plasma of a patient treated with irinotecan and PHY906 using liquid chromatography/tandem mass spectrometry (LC/MS/MS), J. Chromatogr. A 1217 (2010) 5785–5793.
[30] X.F. Chen, H.T Wu, G.G. Tan, et al., Liquid chromatography coupled with time-of-flight and ion trap mass spectrometry for qualitative analysis of herbal medicines, J. Pharm. Anal. 1 (2011) 235–245.